INFLUENCE OF TEMPERATURE ON HUMIDITY SENSOR BASED ON PURE TIN DIOXIDE

Abstract

The powder form of nanoparticles of tin dioxide (SnO_2) was synthesized *via* the co-precipitation technique. The resultant powder was annealed at 500 and 700 °C and fabricated into pellets for moisture-sensing characteristics. The characterization techniques like X-ray diffraction (XRD), field emission scanning electron microscopy (FE-SEM) and the four-probe technique revealed that the nanoparticles have tetragonal structure, nanosphere-like morphology and an electrical band gap, respectively. The crystallite size and particle size of the nanoparticles increased with an increase in annealing temperature from 500 °C to 700 °C. The nanomaterials of SnO_2 showed a sensitivity of 18.76 MΩ/%RH. The hysteresis of the sample was found to decrease with an increase in annealing temperature. The nanomaterial annealed at 700 °C showed 1.8% hysteresis. The nanomaterial SnO_2 was found to be a potential candidate for a humidity sensor operable at room temperature.

Keywords: Humidity Sensor, Nanomaterials, Pellets, Temperature and Hysteresis.

Authors

Neetu Yadav
Department of Physics
University of Lucknow
Lucknow, Uttar Pradesh, India.

Narendra Kumar Pandey
Department of Physics
University of Lucknow
Lucknow, Uttar Pradesh, India.

Vernica Verma
Department of Physics
University of Lucknow
Lucknow, Uttar Pradesh, India.
Peramjeet Singh

Dr. Peramjeet Singh
Department of Physics
University of Lucknow
Lucknow, Uttar Pradesh, India.

Amit Kumar Verma
Department of Physics
University of Lucknow
Lucknow, Uttar Pradesh, India.

Copyright © 2024 Authors

I. INTRODUCTION

Sensors have attracted researchers' attention for the past few years and nanomaterials help them achieve the desired sensor device fabrication. In the range of devices based on transition metal oxides, sensors such as SnO_2, TiO_2, $WO_3$and MoO_3 support advanced humidity sensitivity and better processing techniques. Kucheyev et al. fabricated 3D SnO_2 nanomaterials and reported that SnO_2 is an n-type semiconductor oxide with a large band gap of 3.6 eV [1]. The SnO_2 nanomaterials-based sensor showed better sensitivity and a quick response to relative humidity (RH) in the air at room temperature [2]. P. Singh et al. fabricated MoO_3 samples by the hydrothermal technique and fabricated them into thin films at different temperatures for studying humidity and liquefied petroleum gas sensing properties at room temperature.

They reported that the thin film synthesized at a higher annealing temperature showed better sensitivity with a minimum response and recovery time [3]. Tin dioxide can be synthesized by electron beam evaporation [4], sol-gel process [5], pulse laser deposition [6], molecular beam epitaxy [7] and hydrothermal technique [8]. Timofeev et al. studied information regarding point defects and the impact of flow rate on the structure and elemental composition of synthesized tin oxide thin films [9].

The morphology of the synthesized nanomaterials depends on the synthesis techniques and whether they are fabricated as nanorods, nanotubes, nanoflowers, *etc*. Depending on their morphologies, they showed different sensing responses and various applications. Compared to other oxides, SnO_2 metal oxide has a good agreement with humidity sensing because of its uncomplicated structure [10], reasonable cost, better selectivity[11], and oxygen vacancies. Apart from humidity sensors, SnO_2 has other applications such as lithium-ion batteries [12], supercapacitors [13], gas sensors [14], transparent conductive films [15] and catalysts [16].

The current work focused on the synthesis of tin dioxide nanomaterials and studied the structural, surface, electrical and humidity sensing characteristics of samples annealed at 500 °C and 700 °C.

II. EXPERIMENTS AND RESULTS

1. **Powder Synthesis:** The nanopowder of SnO_2 was prepared using $SnCl_2.2H_2O$ (99.8%, Sigma Aldrich) as a precursor, which was then dissolved in 50 ml of ethanol under constant stirring for 1 hr. The homogeneous solution was adjusted to pH 8 using dropwise ammonium hydroxide. The obtained solution was centrifuged and washed several times with deionized water to obtain the required precipitate. The obtained precipitate was dried at 80 °C under vacuum for 4 hours and finally annealed at 500 °C and 700 °C for 1 hour.

2. **X-ray Diffraction Analysis:** The X-ray Ultima IV diffractometer radiating $CuK_{\alpha 1}$ radiation with a 1.5406 Å wavelength was used for the diffraction analysis of powdered samples with a scanning rate of 0.02 deg./sec and a range of 20 to 70 deg. The diffraction peaks of SnO_2 were observed at (110), (101), (200), (111), (211), (220), (002), (310), (112) and (301) matched the tetragonal structure of SnO_2 (JCPDS No. 01-0657). Debye Scherrer's formula was used to determine the average crystallite size in the following way[17]:

Copyright © 2024 Authors

$$D = \frac{0.9\lambda}{\beta cos\theta} \quad (1)$$

where; D denotes the crystallite size (nm), λ denotes the wavelength (nm), β is the full-width half maximum (radians) and θ denotes the Bragg's angle (radians).

The calculated average crystallite size for samples annealed at 500 °C and 700 °C was 14.402 nm and 30.936 nm, respectively.

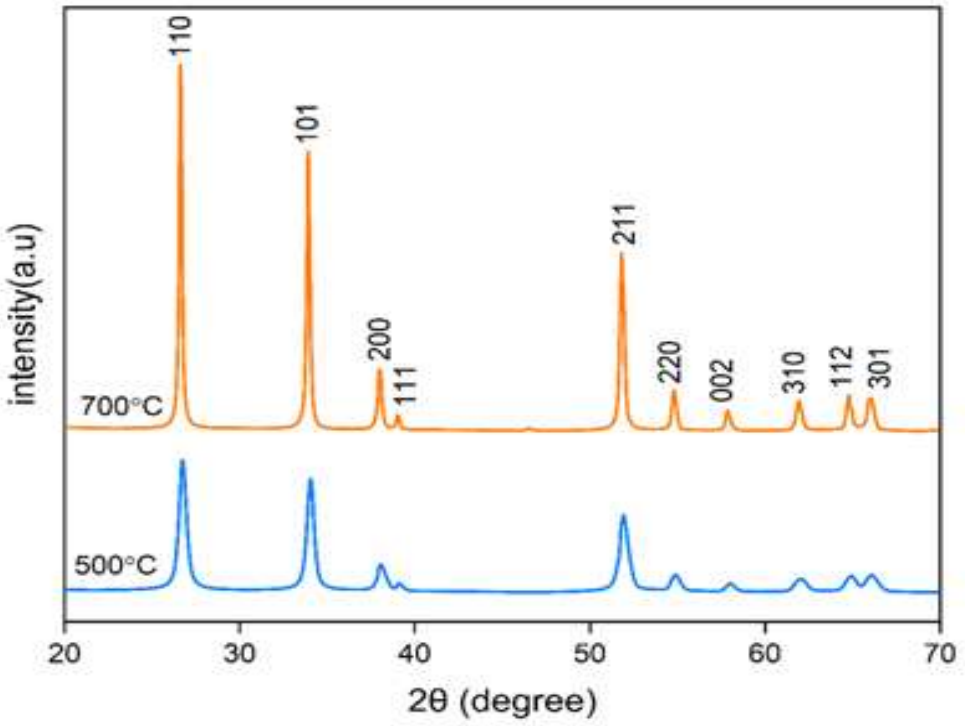

Figure 1: X-ray Spectra of Annealed at 500 and 700°C SnO_2 Nanopowder.

3. **FE-SEM Analysis:** The field emission scanning electron microscopy (FE-SEM) technique investigates the surface morphology of the synthesized samples of SnO_2. The FE-SEM images of the synthesized sample may be nanoflowers, nanobelts, nanorods, nanospheres, nanoballs, *etc*. and can also be used to calculate the particle size. The prepared SnO_2 samples in powder form, annealed at two different temperatures of 500 °C and 700 °C, were investigated by FE-SEM. The FE-SEM images confirm that annealed samples have a nanosphere-like structure with different particle sizes.

The average particle size for the sample annealed at 500 °C and 700 °C was found to be 39.019 nm and 63.923 nm, respectively. The results indicate that as the temperature rose, the particle size also increased due to the agglomeration of large nanoclusters from tiny nanoparticles.

Copyright © 2024 Authors

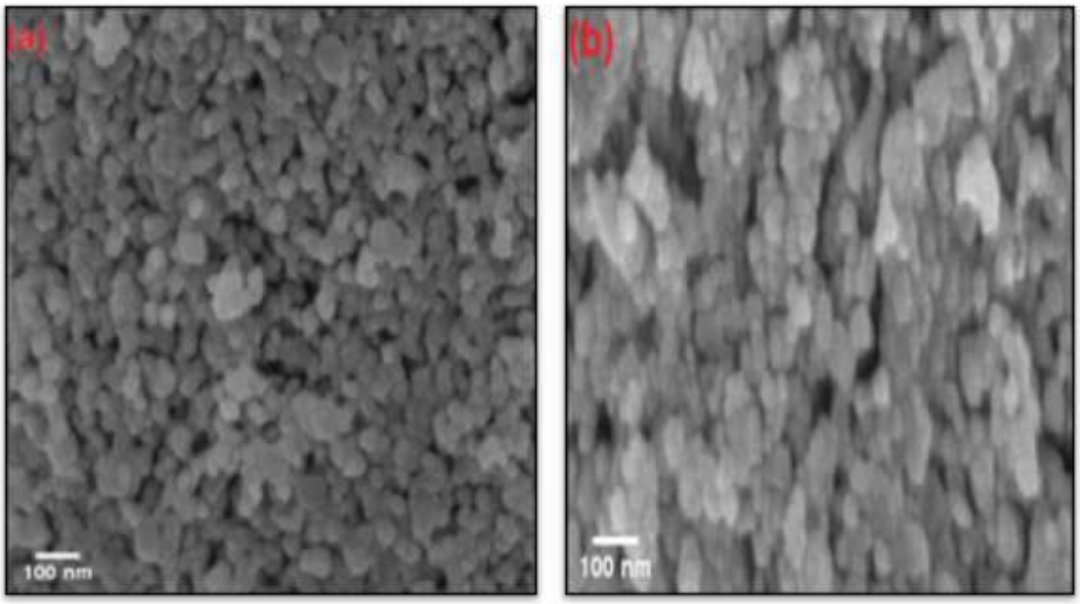

Figure 2: FE-SEM of SnO_2 sample annealed at (a) 500°C and (b) 700°C.

4. **Activation Energy:** The activation energy of SnO_2 samples annealed at two temperatures, 500 °C and 700 °C, was measured using the four-probe method. The Arrhenius equation was used to determine the conductivity of an n-type semiconductor;

$$\sigma = \sigma_o e^{\frac{-\Delta E}{2kT}} \quad (2)$$

where;σ represents the conductivity at an absolute temperature $(\Omega\ cm)^{-1}$, σ_o denotes the constant term, ΔE is activation energy (eV), T is the absolute temperature (Kelvin)and k represents the Boltzmann constant $(8.6\times10^{-5}\ eVK^{-1})$.

On taking log both sides, we got;

$$ln\sigma = ln\sigma_o - \frac{\Delta E}{2k\times10^3}\frac{1000}{T} \quad (3)$$

$$\Delta E = -(2 \times 8.6 \times 10^{-2} \times slope)\ eV \quad (4)$$

The activation energy of the synthesized samples was obtained by the slope of the plot between1000/T and ln σ.

Copyright © 2024 Authors

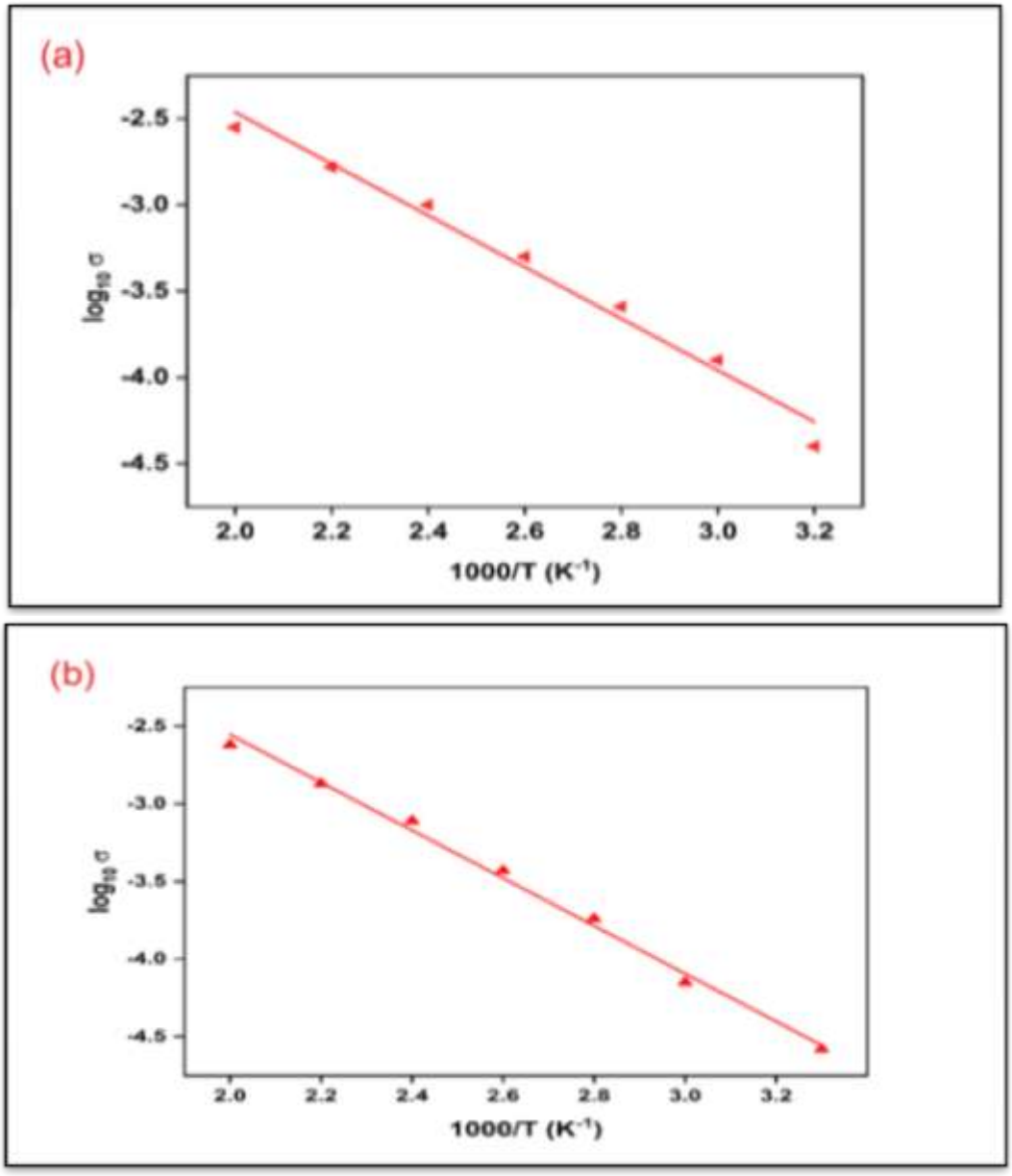

Figure 3: Activation Plot of the Synthesized Sample at (a). 500°C and (b). 700 °C for 1000/T vs. log σ.

The above Fig. 3 indicates that the electrical conductivity of the sample depends on temperature and as the annealing temperature increases or decreases, the electrical conductivity of the semiconductor varies accordingly. It was observed from the calculation that as the annealing temperature increased from 500 °C to 700 °C, the activation energy decreased from 0.326 to 0.278 eV, which indicates the increase in electrical conductivity of the samples.

III. HUMIDITY SENSING STUDIES

To study the humidity-sensing behavior of the SnO_2 material, a set-up was installed that consists of a resistance meter and a hygrometer. The humidity sensing characteristics

Copyright © 2024 Authors

were studied for both samples annealed at 500 °C and 700 °Cand relative humidity was determined in terms of variation in the resistance meter at room temperature. For better humidity sensing characteristics, nanomaterials should have a wide surface area with reduced particle size because the sensor relies on electronic conduction. Tin possesses the 4^+ valance ions that have a vacant 5p shell (p^0 oxide) in tin dioxide. This indicates that there are no cations accessible for adsorption. Dissociative chemisorption is a reason for the adsorption of water molecules on the surface of the oxide and it was noticed that when the relative humidity of SnO_2 increases from 10 to 90%, the resistance decreases to the minimum value. Fig. 4 represents the humidity graph between relative humidity (%RH) and resistance (MΩ).

We noticed a quick decline in resistance in the range of 10-45 %RH; whereas its decline became slow in the range of 45-90 %RH. Due to the large number of available electrons in SnO_2, the resistance decreases with an increase in relative humidity. With an increase in relative humidity, the moisture starts condensing on the surface of the sample, which decreases the resultant resistance.

1. **Sensitivity:** Sensitivity can be calculated by dividing the variation in resistance by the variation in relative humidity in the range of 10–90 %RH. The sensitivity of the sensing elements was determined by the average of all the estimated values. The equation used to calculate the sensitivity is given below:

$$Sensitivity\ (\%) = \frac{\Delta R}{\Delta RH} \qquad (5)$$

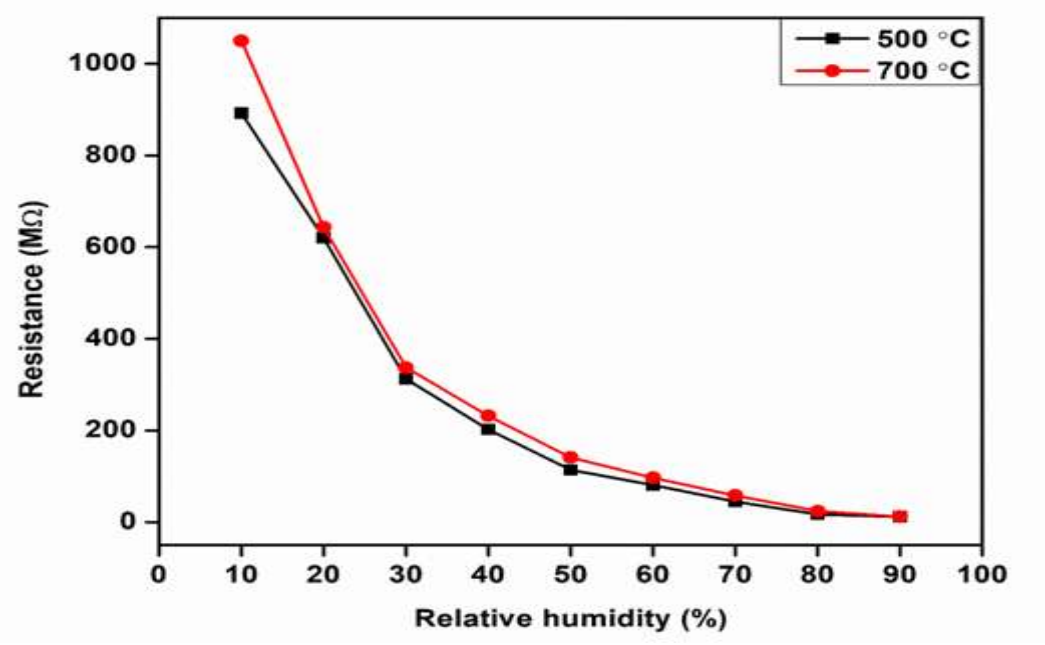

Figure 4: Humidification Graph of SnO_2 Annealed at two Temperatures 500 °C and 700 °C.

From the above equation, the obtained sensitivity (%) was 18.46 and 18.76 for the samples annealed at 500 and 700 °C, respectively.

2. **Hysteresis:** One aspect of a sensor's performance comprises hysteresis. Researchers focussed on the sensor types with the least possible hysteresis value. It is referred to as the resistance lag that occurs during physisorption and chemisorption [18]. The hysteresis

Copyright © 2024 Authors

plot of two samples annealed at 500 °C and 700 °C was examined and shown in figs 5 (a) and (b), respectively. It was observed that, with an increase in annealing temperature, there is a decrease in the value of hysteresis. The average calculated value of hysteresis for the sample annealed at 500 °C was found to be 2.14%, whereas it decreased to 1.8% for the sample annealed at 700 °C. As we increase the annealing temperature, the hysteresis decreases due to poor electron transport at the interfaces of the sensor [19].

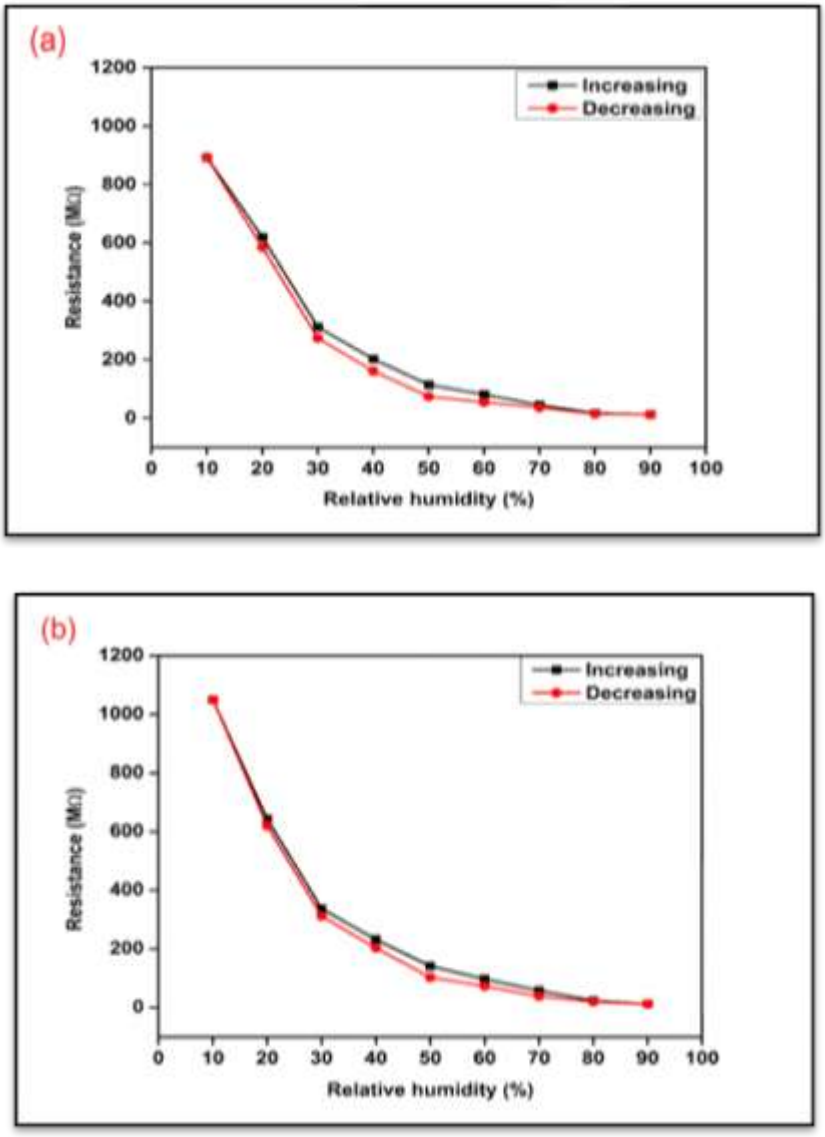

Figure 5: Hysteresis graph of SnO_2 at (a) 500 °C and (b)700°C.

IV. CONCLUSION

The powder form of SnO_2 nanomaterial was synthesized by using the co-precipitation technique and annealed at two temperatures: 500 °C and 700°C. As we increased the annealing temperature, the crystallite size was found to increase, as confirmed by X-RD results. The FE-Sem image confirms that the particle size increases with an increase in annealing temperature. There was a decrement in the activation energy obtained by the four-

Copyright © 2024 Authors

probe method, which is indirectly proportional to electrical conductivity. The humidity sensing characteristics confirm that the sensitivity increases from 18.46% to 18.76% and that the hysteresis value of synthesized samples decreases as the temperature increases.

V. ACKNOWLEDGMENT

The authors are grateful to Prof. R.K. Shukla for providing X-RD facility, department of physics, university of Lucknow and Dr. Subodh for providing FE-SEM facility, BSIP, Lucknow.

Author Contribution: All authors contributed equally in the presented work.

REFERENCES

[1] S.O. Kucheyev, T.F. Baumann, P.A. Sterne, Y.M. Wang, T.V. Buuren, A.V. Hamza, L.J. Terminello and T.M. Willey, "Surface electronic states in three- dimensional SnO_2 nanostructures", Physical Review B. (2005). https://doi.org/10.1103/PhysRevB.72.035404.

[2] Q. Kuang, C. Lao, Z.L Wang, Z. Xie and L. Zheng, "High sensitivity humidity sensor based on a single SnO_2 nanowire", Journal of the American Chemical Society, (2007). https://doi.org/10.1021/ja070788m

[3] P. Singh, N.K. Pandey, V.S. Kumar, V. Verma, A. Singh, P. Gupta and B.C. Yadav, "Highly sensitive pure molybdenum trioxide thin films at a higher annealing temperature for liquefied petroleum gas and humidity sensing at room temperature", Applied Physics A. (2023). https://doi.org/10.1007/s00339-023-06491-7

[4] A.F. Khan, M. Mehmood, M. Aslam and M. Ashraf, "Characteristics of electron beam evaporated nanocrystalline SnO2 thin films annealed in air", Applied Surface Science, (2010). https://doi.org/10.1016/j.apsusc.2009.10.047

[5] T.M. Racheva and G.W. Critchlow, "SnO_2 thin films prepared by the sol-gel process", Thin Solid Films, (1997). https://doi.org/10.1016/S0040-6090(96)08956-0.

[6] H. Kim, R.C.Y. Auyeung and A. Piqué, "Transparent conducting F-doped SnO_2 thin films grown by pulsed laser deposition"

[7] Thin solid films, (2008). https://doi.org/10.1016/j.tsf.2007.11.079.
M. Batzill, J.M. Burst and U. Diebold, "Pure and cobalt-doped SnO_2(101) films grown by molecular beam epitaxy on Al_2O_3",Thin Solid Films, (2005). https://doi.org/10.1016/j.tsf.2005.02.016.

[8] O. Lupan, L. Chow, G. Chai, A. Schulte, S. Park and H. Heinrich, "A rapid hydrothermal synthesis of rutile SnO_2 nanowires", Materials Science and Engineering: B, (2009). https://doi.org/10.1016/j.mseb.2008.12.035

[9] V.A.Timofeev, V.I. Mashanov, A.I. Nikiforov,I.A. Azarov,I.D. Loshkarev, I.V. Korolkov,T.A. Gavrilova, M.Y. Yesin and I.A.Chetyrin, "Effect of annealing temperature on the morphology, structure and optical properties of nanostructured SnO(x) films",Materials Research Express, (2020). 10.1088/2053-1591/ab6122

[10] Akgul, F. Aksoy, C. Gumus, O. Er Ali, A. H. Farha, G. Akgul, Y. Ufuktepe, and Z. Liu. "Structural and electronic properties of SnO2." Journal of Alloys and Compounds 579 (2013): 50-56. https://doi.org/10.1016/j.jallcom.2013.05.057

[11] S. Syreina, J. - H. Lee, D. - H. Yang, M. Weber, I. Iatsunskyi, E. Coy, A. Razzouk, S. S. Kim, and M. Bechelany. "Humidity-resistant gas sensors based on SnO2 nanowires coated with a porous alumina nanomembrane by molecular layer deposition." Sensors and Actuators B: Chemical 344 (2021): 130302. https://doi.org/10.1016/j.snb.2021.130302

[12] J.S. Chen and X.W. Lou, "SnO_2-Based Nanomaterials: Synthesis and Application in Lithium-Ion Batteries", Small, (2013). https://doi.org/10.1002/smll.201202601

Copyright © 2024 Authors

[13] Z.A Hu, Y.L. Xie, Y.X. Wang, L.P.Mo, Y.Y. Yang and Z.Y. Zhang, "Polyaniline/SnO_2 nanocomposite for supercapacitor applications", Materials Chemistry and Physics, (2009). https://doi.org/10.1016/j.matchemphys.2008.11.005

[14] G. Zhang and M. Liu, "Effect of particle size and dopant on properties of SnO_2-based gas sensors", Sensors and Actuators B: Chemical, (2000). https://doi.org/10.1016/S0925-4005(00)00528-1

[15] M.-M. Bagheri-Mohagheghi and M.S. -Saremi, "The influence of Al doping on the electrical, optical and structural properties of SnO_2 transparent conducting films deposited by the spray pyrolysis technique", Journal of Physics D: Applied Physics, (2004). 10.1088/0022-3727/37/8/014

[16] M.K. Lam and K.T. Lee, "Mixed methanol–ethanol technology to produce greener biodiesel from waste cooking oil: A breakthrough for $SO_42-/SnO_2–SiO_2$ catalyst", Fuel Processing Technology, (2011). https://doi.org/10.1016/j.fuproc.2011.04.012

[17] T.A. Saleh, Polymer Hybrid Materials and Nanocomposites, Fundamentals and Applications, Plastics Design Library (2021) 213–240, https://doi.org/10.1016/B978-0-12-813294-4.00005-4

[18] H. Parangusan, J. Bhadra, Z. Ahmad, S. Mallick, F. Touati and N. Al-Thani, "Humidity sensor based on poly (lactic acid)/PANI–ZnO composite electrospun fibers", RSC advances, (2021). 10.1039/D1RA02842A

[19] J. Barbé, M.L. Tietze, M. Neophytou, B. Murali, E. Alarousu, A.E. Labban, M. Abulikemu, W. Yue, O.F. Mohammed, I. McCulloch and A.Amassian, "Amorphous Tin Oxide as a Low-Temperature-Processed Electron-Transport Layer for Organic and Hybrid Perovskite Solar Cells", ACS applied materials & interfaces, (2017). https://doi.org/10.1021/acsami.6b13675

Copyright © 2024 Authors